Direction of Arrival Estimation of Spread Spectrum Signal

Hongwei Zhao(✉) and Zichun Zhang

School of Electronics and Information, Northwestern Polytechnical University, Xi'an 710072, China
hongvi_zhao@126.com, 2244247525@qq.com

Abstract. The sensor networking based on multi-source information fusion can significantly improve direction accuracy, and the sensor networking is always used in direction of spread spectrum signals. Aimed at eliminating the phase ambiguity of the phase-comparison method, this paper proposed a direction-finding method based on ISM (Incoherent Signal Subspace Method) and CSM (Coherent Signal Subspace Method) algorithms. Firstly, the wideband spread spectrum signal is divided into narrowband at different time points. Then perform the DCT (Discrete Cosine Transform) and obtain the covariance matrix at different frequency points. Finally, the narrowband signal power spectrums at independent frequency points are synthesized to obtain the total power spectrum of spread spectrum signal. The simulation results demonstrate that the ISM and CSM algorithms can accurately determine the direction of the spread spectrum signal, and the direction error is kept within 1° when the signal-to-noise ratio (SNR) is higher than 5 dB, which satisfy the accurate direction-finding requirement. Therefore, the ISM and CSM algorithms based on sensor networking is a necessary solution in high-precision direction of spread spectrum signals.

Keywords: Spread spectrum signal · DOA · ISM · CSM

1 Introduction

The DOA (direction of arrival) of the signal based on multi-source information fusion can significantly improve direction accuracy, and the multi-source information is always obtained through sensor networking. The spread spectrum signal has good anti-interference, low interception and strong networking capability, and it is widely used in military communication and GNSS navigation and positioning [1, 2]. It directly modulates the information code through a pseudo-random spread spectrum sequence, so that the used bandwidth of the transmission signal is greatly increased. For the signal transmitter, since the energy of transmitting information is extended to a wider spectrum, the signal radiated power per unit bandwidth is reduced, and the system capacity is improved [3]. For the cooperative receiver, the received signal increases the anti-interference ability of the system. Because the signal is despreaded by the known spread spectrum sequence,

B. Li et al. (Eds.): IoTaaS 2019, LNICST 316, pp. 589–597, 2020.
https://doi.org/10.1007/978-3-030-44751-9_50

and the channel noise and the narrowband interference signal are extended to a wider frequency band [4].

The estimation of the DOA of the spread spectrum signal plays an important role in various military and civilian fields such as GNSS and GPS navigation, as well as sonar and radar. The spread spectrum signal is essentially a wideband signal. Compared with wideband DOA, the narrowband DOA estimation algorithm developed earlier [5]. In 1967, Burg proposed the MEM algorithm (Maximum Entropy Method) and 1969 Capon proposed the MVM algorithm (Minimum Variance Method). In these methods, the resolution ratio and accuracy of DOA estimation are improved, but in low signal-to-noise ratio the estimation performance is not good, and the high resolution in the true sense is not realized [6, 7]. The classification algorithm appeared in the 1970s, such as the MUSIC algorithm (Multiple Signal Classification) proposed by Schmidt in 1979 [8, 9]. It is the first algorithm to realize signal DOA estimation by using subspace. The resolution ratio of the array signal direction-finding is greatly improved, and it is an important node in the history of high resolution ratio direction-finding algorithm [10, 11]. The broadband high-resolution direction-finding algorithm is developed on the basis of narrowband signal direction-finding algorithm. The DOA estimation of narrow-band signals has been developed for several decades, and the technology has been relatively mature [12, 13]. However, direction-finding algorithm for wideband signals, especially for spread-spectrum signals, there are few studies on DOA estimation. The existed direction-finding technology of wideband signals is mainly based on the phase comparison method [14, 15]. However, in the phase comparison method, the phase ambiguity occurs with a period of multiple of 2π and it is difficult to eliminate, which limits the direction-finding accuracy [16, 17]. In this paper, aiming at solving the above problems, this paper proposes the ISM (Incoherent Signal Subspace Method) and CSM (Coherent Signal Subspace Method) methods to determine the direction of the wideband spread spectrum signal.

2 DOA Estimation

2.1 Mathematical Model of the Signal

In the narrowband signal model, a phase delay is used to approximately represent the time delay, which is obviously no longer applicable for wideband signals. In this case, Fourier transform is used. Each wideband signal is distributed within $[\omega_L, \omega_H]$ and use the following formula to express the output of the m element:

$$x_m(t) = \sum_{l=1}^{P} \alpha_l s_l(t - \tau_{lm}) + n_m(t), m = 1, 2, \cdots, M \tag{1}$$

Where, α_l is the gain of the m th element for the l th signal; $n_m(t)$ is additive noise at the m th element; τ_{lm} is the delay generated by the m th signal when it reaches the l th element.

For the uniform linear array; $\tau_{lm} = \nu_m \sin\theta_l$, $\nu_m = d_m/c$; d is the array space; c is the speed of the signal in the propagation medium; θ_i is the target angle to estimate. Assuming α_l is 1, and the array is sampled at time t. The output vector of the array is as follows:

$$X(t) = \begin{bmatrix} \sum_{l=1}^{P} s_l(t - \tau_{l1}) \\ \sum_{l=1}^{P} s_l(t - \tau_{l2}) \\ \vdots \\ \sum_{l=1}^{P} s_l(t - \tau_{lM}) \end{bmatrix} + \begin{bmatrix} n_1(t) \\ n_2(t) \\ \vdots \\ n_M(t) \end{bmatrix} \tag{2}$$

Adopt DFT for Eq. (1), we can get:

$$X_m(\omega) = \sum_{l=1}^{P} S_l(\omega) \exp(-j\omega\tau_{lm}) + N_m(\omega) \tag{3}$$

When the frequency is f_n, rewrite the above equation into a matrix equation:

$$X(f_n) = A(f_n)S(f_n) + N(f_n) \tag{4}$$

Where, $A(f_n)$ is $M \times P$ matrix, represents a flow matrix of the spatial array.

$$\begin{aligned} X(f_n) &= \left[X_1(f_n)\ X_2(f_n) \cdots X_M(f_n) \right]^T \\ N(f_n) &= \left[N_1(f_n)\ N_2(f_n) \cdots N_M(f_n) \right]^T \\ S(f_n) &= \left[S_1(f_n)\ S_2(f_n) \cdots S_P(f_n) \right]^T \end{aligned} \tag{5}$$

$$A(f_n) = \begin{bmatrix} \exp(-j2\pi f_n \tau_{11}) & \exp(-j2\pi f_n \tau_{12}) & \cdots & \exp(-j2\pi f_n \tau_{1P}) \\ \exp(-j2\pi f_n \tau_{21}) & \exp(-j2\pi f_n \tau_{22}) & \cdots & \exp(-j2\pi f_n \tau_{2P}) \\ \vdots & \vdots & \ddots & \vdots \\ \exp(-j2\pi f_n \tau_{M1}) & \exp(-j2\pi f_n \tau_{M2}) & \cdots & \exp(-j2\pi f_n \tau_{MP}) \end{bmatrix} \tag{6}$$

The covariance matrix corresponding to Eq. (4) is as follows:

$$\begin{aligned} R(f_n) &= A(f_n)E\left[S(f_n)S^H(f_n) \right] A^H(f_n) + {\sigma_n}^2 I \\ &= A(f_n)R_s(f_n)A^H(f_n) + {\sigma_n}^2 I \end{aligned} \tag{7}$$

It is represented at different frequency points. Where, $R_s(f_n) = E\left[S(f_n)S^H(f_n)\right]$ represents the covariance matrix of the wideband signal at f_n.

2.2 ISM (Incoherent Signal Subspace Method)

From Eq. (7), we obtain the covariance matrix $R(f_n)$ of the wideband signal. During this part, the wideband signals involved are incoherent wideband signals. Assuming there are J frequency points in the signal bandwidth, and the covariance matrix is $R(f_j)$, $j = 1, 2, \cdots, J$. Decompose this matrix to obtain the M eigenvalues: $\lambda_1(f_j) \geq \lambda_2(f_j) \geq \cdots \geq \lambda_M(f_j)$ in descending order and the corresponding eigenvectors is $e_m(f_j), m = 1, 2, \cdots M$. The eigenvectors corresponding to the large P eigenvalues and the eigenvectors corresponding to the small $M - P$ eigenvalues are constructed into matrixes respectively.

$$\begin{aligned} US(f_j) &= [e_1(f_j), e_2(f_j), \cdots, e_P(f_j)] \\ UN(f_j) &= [e_{P+1}(f_j), e_{P+2}(f_j), \cdots, e_M(f_j)] \end{aligned} \tag{8}$$

The signal subspace constructed at f_j is the same as the space formed by the array flow matrix, and the signal subspace is orthogonal to the noise subspace. That is, $span\{U_S(f_j)\} = span\{A(f_j, \theta)\} span\{U_S(f_j)\} \perp span\{U_N(f_j)\}$.

We can firstly obtain the covariance matrix of each frequency point in the bandwidth of the wideband signal. Then the weighted average of these spatial spectrum is obtained to get the total ISM spatial spectrum. Finally, DOA estimation is performed. There are two different weighted averaging methods: the arithmetic averaging method and the geometric averaging method. The arithmetic average method calculates the ISM spatial spectrum:

$$P_{ISSM1}(\theta) = \left(\frac{1}{J} \sum_{j=1}^{1} \frac{1}{P_{MUSIC}(f_j, \theta)} \right)^{-1} \tag{9}$$

The geometric mean method calculates the ISM spatial spectrum:

$$P_{ISSM2}(\theta) = \left(\prod_{j=1}^{J} \frac{1}{P_{MUSIC}(f_j, \theta)} \right)^{-\frac{1}{J}} \tag{10}$$

Here, $P_{MUSIC}(f_j, \theta)$ represents the MUSIC spatial spectrum at j th frequency:

$$P_{MUSIC}(f_j, \theta) = \frac{1}{a^H(f_j, \theta) U_n(f_j) U_n^H(f_j) a(f_j, \theta)} \tag{11}$$

2.3 CSM (Coherent Signal Subspace Method)

In ISM algorithm for wideband DOA estimation, we need to select the frequency point with high SNR, and also carry out plenty of snapshots. In this case, the DOA calculation is greatly increased. Besides, the ISM algorithm cannot perform in DOA estimation of coherent wideband signals. The CSM algorithm constructs a focusing matrix by aligning the array flow matrix of each frequency point at the predicted angle to the same array flow matrix at the focus frequency. Then the array covariance matrix corresponding to each frequency of the signal is focused transform under this focus matrix.

Assuming $s_1(t)$ and $s_2(t)$ $(s_2(t) = s_1(t - t_0))$ are two coherent broadband signals, let $s(t) = \begin{bmatrix} s_1(t) \\ s_2(t) \end{bmatrix}$ and its covariance matrix can be expressed as:

$$\begin{aligned} R_s(\tau) &= E\left\{s(t)s^H(t+\tau)\right\} \\ &= \begin{bmatrix} R_1(\tau) & R_1(\tau - t_0) \\ R_1(\tau + t_0) & R_1(\tau) \end{bmatrix} \end{aligned} \tag{12}$$

Where, $R_1(\tau)$ is the correlation function of $s_1(t)$. The spectral matrix can be obtained by performing a Fourier transform on both sides of the above formula:

$$P_s(f) = \begin{bmatrix} P_1(f) & P_1(f)\exp(-j2\pi f t_0) \\ P_1(f)\exp(j2\pi f t_0) & P_1(f) \end{bmatrix} \tag{13}$$

The spectral matrix $P_s(f)$ of $s_1(t)$ is always a singular matrix and the signal subspace and the noise subspace cannot be completely orthogonal. In order to solve this problem, it needs to make $P_s(f)$ be non-singular. Smoothing the spectral matrices in frequency at individual J frequency points:

$$\begin{aligned} P(f) &= \frac{1}{J}\sum_{j=1}^{J} P(f_j) \\ &= \begin{bmatrix} P(f_0) & P(f_0)\frac{1}{J}\sum\limits_{j=1}^{J}\exp(-j2\pi f_j t_0) \\ P(f_0)\frac{1}{J}\sum\limits_{j=1}^{J}\exp(j2\pi f_j t_0) & P(f_0) \end{bmatrix} \end{aligned} \tag{14}$$

The construction of the focusing matrix is described in the following. Assuming that the rank of the array $A(f_j)$ flow matrix at the frequency point f_j is P, the focusing matrix should satisfy:

$$T(f_j)A(f_j) = A(f_0), j = 1, 2, \cdots, J \tag{15}$$

Here, f_0 is the reference frequency and also the focus frequency. $T(f_j)$ is a dimensional non-singular $M \times M$ matrix. Because the rank of $A(f_j)$ and $A(f_0)$ is P, we can construct $M \times (M - P)$ matrixes $B(f_j)$ and $B(f_0)$ to make $[A(f_j)|B(f_j)]$ and $[A(f_0)|B(f_0)]$ be both non-singular matrixes. We can get the focusing matrix as following:

$$T(f_j) = [A(f_0)|B(f_0)][A(f_j)|B(f_j)]^{-1} \tag{16}$$

After the focus matrix transformation, the array output vector is:

$$Y(f_j) = T(f_j)X(f_j) = A(f_0)S(f_j) + T(f_j)N(f_j), j = 1, 2, \cdots, J \tag{17}$$

We can get the following:

$$\sum_{j=1}^{J} w_j \text{cov}\big(Y(f_j)\big) = A(f_0)\left[\sum_{j=1}^{J} w_j P_s(f_j)\right] A^H(f_0) + {\sigma_n}^2 \sum_{j=1}^{J} w_j T(f_j) P_n(f_j) T^H(f_j) \tag{18}$$

Where,

$$\begin{gathered} R = A(f_0) R_s A^H(f_0) + {\sigma_n}^2 R_n \\ R = \sum_{j=1}^{J} w_j \text{cov}\big(Y(f_j)\big) \\ R_s = \sum_{j=1}^{J} w_j P_s(f_j) \\ R_n = \sum_{j=1}^{J} w_j T(f_j) P_n(f_j) T^H(f_j) \end{gathered} \tag{19}$$

w_j is the normalized weighted value, which is proportional to the SNR of the frequency f_j. Here, take it as 1.

Decompose the matrix (R, R_n) to obtain the M eigenvalues: $\lambda_1(f_j) \geq \lambda_2(f_j) \geq \cdots \geq \lambda_M(f_j)$ in descending order and the corresponding eigenvectors is $e_m(f_j), m = 1, 2, \cdots M$. The subspace formed by the column vector of $E_s = [e_1, e_2, \cdots, e_P]$ is called the signal subspace, and the subspace formed by the column vector of $E_n = [e_{P+1}, e_{P+2}, \cdots, e_M]$ is called the noise subspace, and then the signal subspace and the noise subspace are orthogonal to each other.

$$\begin{gathered} \lambda_P = \lambda_{P+1} = \cdots = \lambda \\ A^H(f_0) E_n = 0 \\ {Es}^H R_n E_n = OP \times (M - P) \\ {Es}^H R_s E_s = IP \\ {En}^H R_n E_n = I(M - P) \end{gathered} \tag{20}$$

We can get the CSM spatial spectrum as the following:

$$P_{MUSIC}(f_0, \theta) = \frac{1}{a^H(f_0, \theta) Un(f_0) Un^H(f_0) a(f_0, \theta)} \tag{21}$$

3 Simulation Analysis

3.1 Spatial Spectrum Analysis

The distribution of energy of the target signal in all directions in space is the spatial spectrum. This is a intuitive indicator of the performance of the DOA estimation algorithm. In the experiment, it is assumed that the receiving antenna array is a 10 elements uniform linear array, snapshots are performed 128 times and the array element spacing is half of wavelength. The target wideband spread spectrum signals wave come from 20° and 26°. Perform the ISM and CSM algorithm with signal-to-noise ratio of −5db and 5db respectively and following is the spatial spectrum of ISM and CSM.

It can be seen from Figs. 1 and 2 that the power spectrum formed the peak in 20° and 26°, which are the directions of target signal and it almost maintained nearly zero in other directions. That is both the ISM and CSM algorithms can find the direction of the wideband spread spectrum signals. But in the condition with lower SNR, the ISM impossible to find the direction accurately and the CSM has higher resolution ratio. Besides, with the SNR becoming higher, the power spectrum in the target direction is sharper. In practical engineering applications, the resolution of the peaks can be increased by increasing the number of receiving antenna elements and the number of fast snapshots.

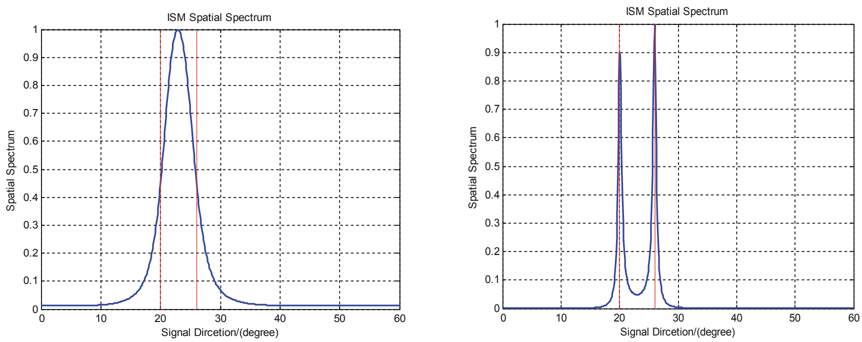

Fig. 1. ISM Spatial Spectrum with SNR of −5 dB and 5 dB.

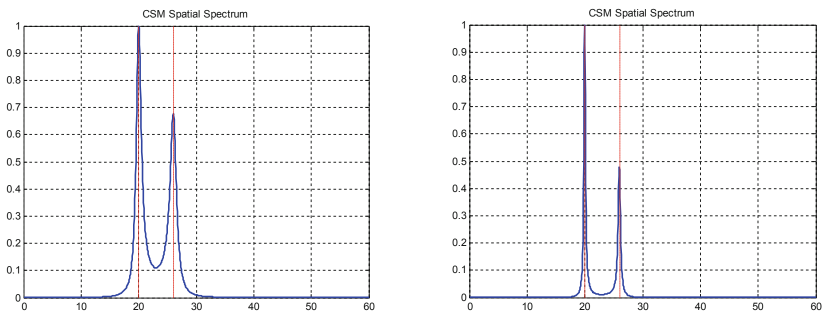

Fig. 2. CSM Spatial Spectrum with SNR of −5 dB and 5 dB.

3.2 Direction Correct Rate

The correct rate of direction-finding refers to the ratio of the number of successful direction-findings to the total number of experiments (monte carlo number). In the experiment, it is assumed that the wideband spread spectrum signals are received by the 10-element antenna. The direction is successfully determined if the difference between the direction-finding angle and the true angle is within 1°. ISM and CSM algorithm are performed 100 monte carlo simulations respectively and following is the result.

It can be seen from Fig. 3 that as the signal-to-noise ratio increases, the direction-finding correct rate of both ISM and CSM algorithms will increase. However, in the case of SNR within −10 dB and 5 dB, the CSM algorithm has a higher direction-finding correct rate. The correct rate of the direction-finding is almost maintained at around 1 after the SNR reaching a certain value. That is, the ISM and CSM direction-finding algorithms proposed in this paper can effectively reduce the influence of interference on the direction-finding result and achieve accurate direction-finding. Therefore, in practical engineering applications, we can use the ISM algorithm for incoherent wideband signals direction and CSM algorithm for coherent wideband signals direction.

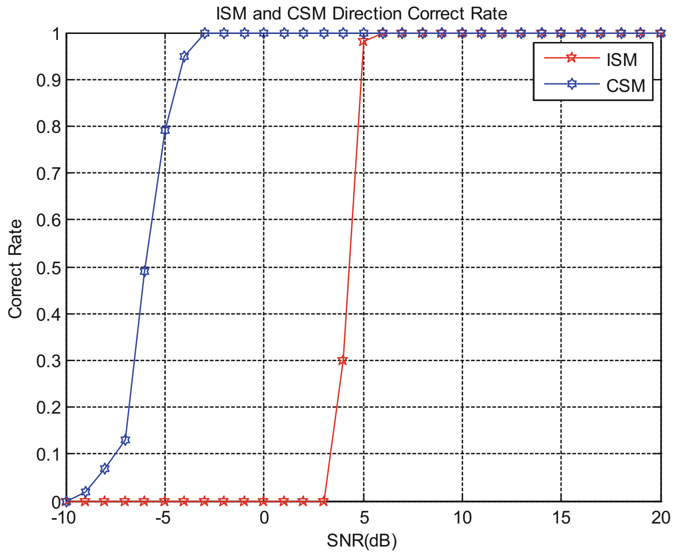

Fig. 3. ISM and CSM Direction Correct Rate.

4 Conclusion

The ISM and CSM algorithms based on sensor networking for the spread spectrum signal direction finding are proposed in this paper. After dividing the received spread spectrum signal into multiple time segments and performing DFT transform, the covariance matrix is obtained at different frequency points according to the different constraint criteria of ISM and CSM. Then, the mentioned covariance matrixes are decomposed into eigenvalues to obtain the corresponding signal subspace and noise subspace. Meanwhile, the narrowband MUSIC direction finding is applied independently at different frequency points. Finally, the geometric power average or arithmetic average method is adopted to synthesize the final power spectrum in order to implement the direction finding of wideband spread spectrum signal. When the SNR is higher than 5 dB, the proposed algorithm performance satisfies accurate and low error direction finding, which should be better for engineering direction finding of spread spectrum signals.

Acknowledgements. This work was supported by the National Natural Science Foundation of China (Grant No. 61771393 and 61571368), and the seed Foundation of Innovation and Creation for Graduate students in Northwestern Polytechnical University.

References

1. Ren, H.P., et al.: A chaotic spread spectrum system for underwater acoustic communication. Physica A Stat. Mech. Appl. **478**, 77–92 (2017)
2. Bo, L.I., Gao, X.G.: Integrated decision for airborne weapon systems based on bayesian networks. J. Syst. Simul. **19**(4), 886–889 (2007)
3. Zhang, Y.-S., et al.: Comb jamming mitigation in frequency-hopping spread spectrum communications via block sparse bayesian learning. Acta Armamentarii **39**(9), 1864–1872 (2018)
4. Park, H.P., Kim, M., Jung, J.H.: Spread-spectrum technique employing phase-shift modulation to reduce EM noise for parallel–series LLC resonant converter. IEEE Trans. Power Electron. **34**(2), 1026–1031 (2018)
5. Yang, T.C., Yang, W.B.: Performance analysis of direct-sequence spread-spectrum underwater acoustic communications with low signal-to-noise-ratio input signals. J. Acoust. Soc. Am. **123**(2), 842 (2008)
6. Cadzow, J.A.: A high resolution direction-of-arrival algorithm for narrow-band coherent and incoherent sources. IEEE Trans. Acoust. Speech Signal Process. **36**(7), 965–979 (1988)
7. Uddin, M.A., et al.: Direction of arrival of narrowband signals based on virtual phased antennas. Communications (2018)
8. Hassen, S.B., et al.: DOA estimation of temporally and spatially correlated narrowband noncircular sources in spatially correlated white noise. IEEE Trans. Signal Process. **59**(9), 4108–4121 (2011)
9. Nunes, L.O., et al.: A steered-response power algorithm employing hierarchical search for acoustic source localization using microphone arrays. IEEE Trans. Signal Process. **62**(19), 5171–5183 (2014)
10. Zhang, D., et al.: Improved DOA estimation algorithm for co-prime linear arrays using root-MUSIC algorithm. Electron. Lett. **53**(18), 1277–1279 (2017)
11. Chen, Z., et al.: A novel noncircular MUSIC algorithm based on the concept of the difference and sum coarray. Sensors **18**(2), 344 (2018)
12. Cui, K.B., et al.: DOA estimation of multiple LFM sources using a STFT-based and FBSS-based MUSIC algorithm. Radioengineering **26**(4), 1126–1137 (2017)
13. Wang, J., et al.: DOA estimation of excavation devices with ELM and MUSIC-based hybrid algorithm. Cogn. Comput. **9**(4), 1–17 (2017)
14. Altarifi, M., Filipovic, D.S.: On the assessment of antenna patterns for wideband amplitude-only direction finding. IEEE Antennas Wireless Propag. Lett. **17**, 385–388 (2018)
15. Lee, J.H., Lee, J., Woo, J.: Method for obtaining three- and four element array spacing for interferometer direction-finding system. IEEE Antennas Wireless Propag. Lett. **15**, 897–900 (2016)
16. Wang, C., Mu, J.: Direction-finding via phase comparison using orthogonally cross dipole antenna. Chin. J. Sci. Instrum. **32**(5), 976–982 (2011)
17. Zhang, T., et al.: Resolving phase ambiguity in dual-echo dixon imaging using a projected power method. Magn. Reson. Med. **77**(5), 2066–2076 (2017)